

Characterization of ZrO₂-Montmorillonite Pillarization Process from Local Zirconium Oxychloride Local Made PSTA-BATAN

Muzakky* and Herry Poernomo

Center for Accelerator Science and Technology - National Nuclear Energy Agency,
Jl. Babarsari No. 21, POB 6101 ykbb, Yogyakarta 55281, Indonesia

Received October 5, 2017; Accepted March 20, 2018

ABSTRACT

Characterization of the pillarization process product of ZrO₂-montmorillonite from Zirconium oxychloride local made of PSTA-BATAN has been done. The objective of this research is to control the quality of pillarization process product of the new material ZrO₂-montmorillonite. This new material was produced from local made Zirconium oxychloride (ZOC) of PSTA-BATAN by dry process and bentonite (Na-montmorillonite) imported from Thailand by the pillarization process. During optimization, the pillarization quality control would be followed by absorbance using Diffuse Reflectance Ultraviolet-Visible (UV-Vis DRS) spectroscopy and X-Ray Diffraction (XRD). While the type of functional group can be detected by Fourier Transform Infrared (FTIR) spectrophotometry, and the surface image was observed by using Transmission Electron Microscopy (TEM) and BET methods. The result gained showed that the optimum quality of ZrO₂-montmorillonite was at Zr concentration of 0.2 M with the absorbance of 1.04 au by XRD and DRS. The best precursor used was ethylene glycol with a drying process in the cold conditions at the absorbance of 1.2 au. The best calcination process was at the temperature of 600 °C with the reached absorbance value of 1.3 au. The results of TEM image observation after calcination at the temperature of 600 °C were clearer and more porous than before and showed specific surface area of 105 m²/g. The interpretation results of FTIR spectra on the new material of ZrO₂-montmorillonite contained the cluster of ≡Si-OH, ≡Al-OH and Si-O functional groups indicating pillar groups.

Keywords: UV-Vis DRS; FTIR; ZrO₂-montmorillonite; TEM

ABSTRAK

Telah dilakukan karakterisasi hasil proses pilarisasi ZrO₂-montmorilonit dari zirkonium oksiklorid lokal buatan PSTA-BATAN. Tujuan dari penelitian ini adalah melakukan kontrol kualitas terhadap hasil proses pilarisasi pada pembuatan material baru ZrO₂-montmorilonit. Material baru ini dibuat berbahan dasar zirkonium oksiklorid (ZOC) lokal buatan PSTA-BATAN memakai proses kering dan bentonit (Na-montmorilonit) impor dari Thailand melalui proses pilarisasi. Selama optimasi kontrol kualitas pilarisasi akan diikuti oleh aborbansi menggunakan UV-Vis DRS dan XRD. Sedangkan jenis gugus fungsi akan dideteksi dengan FTIR, dan citra permukaan diamati menggunakan Transmission Electron Microscopy (TEM) dan BET. Hasil didapat bahwa kualitas gugus fungsi ZrO₂-montmorilonit optimal pada konsentrasi Zr 0,2 M dengan absorbansi 1,04 au dengan XRD dan DRS. Prekursor terbaik menggunakan etilen glikol dengan proses pengeringan pada keadaan dingin dengan absorbansi 1,2 au. Proses kalsinasi terbaik pada suhu 600 °C dengan nilai absorbansi mencapai 1,3 au dan harga spesifik surface area 105 m²/g. Hasil pengamatan citra TEM setelah kalsinasi pada suhu 600 °C tampak lebih terang dan berporous daripada sebelumnya. Hasil interpretasi dengan FTIR pada bahan baru ZrO₂-montmorilonit mengandung gugus fungsi group ≡Si-OH, ≡Al-OH dan Si-O yang merupakan kelompok pilar.

Kata Kunci: UV-Vis DRS; FTIR; ZrO₂-montmorilonit; TEM

INTRODUCTION

Center for Accelerator Science and Technology (PSTA)-BATAN by means of DIPA (List of Budget Implementation) program and INSINAS (Research Incentive of National Innovation System) has successfully processed zircon concentrate into several superior products of zircon mineral based. Such

excellent products, as Zr-opacifier, ZrOCl₂ (ZOC) and ZrO₂ (zirconia) [1] One of the implementations of the Regulation of the Minister of Energy and Mineral Resources No. 51 of 2017 about the Increase of Mineral Added Value through Mineral Processing and Purification Activity, PSTA-BATAN has contributed in making prototype of ZOC products from the raw material of local zircon concentrate (Kalimantan) [1]. As

* Corresponding author.
Email address : muzakkyi@batan.go.id

a follow up of the implementation of Minister Regulation (Permen ESDM) No. 5 of 2017, the author made an effort to enhance the added value of ZOC to become new materials of ZrO₂-montmorillonite. Montmorillonite mineral is widely found in some areas such as in Gunung Kidul district and it could be obtained by importing from Thailand with a cheaper price [2] The quality of pillarization is urgently understood in the application of ZrO₂-montmorillonite as an adsorbent, catalyst and semiconductor materials so that it is very interesting as the research topic for being conducted. The new material ZrO₂-montmorillonite is widely used in catalysts for several organic processes, especially oil refining (hydrotreating, hydrocracking, and catalytic), and has been widely synthesized by some authors using ZOC made in some industrial products.

Mnasri's research [3] that synthesized zirconia-pillared bentonite using Merck-made ZOC. Then Watimah has performed a synthesis of zirconia-pillared along with her derivatives also using ZOC made by Merck [4-8]. Furthermore, Utubira [9] has synthesized zirconia-pillared bentonite using ZOC product of E Merck, but Bahranowski [10] synthesized [Ti, Zr] -pillared montmorillonite used products from Fluka Switzerland. Another study conducted by Suseno [11] has also synthesized Zirconia pillared bentonite using ZOC Merck-product, while Chaabene [12] used Sigma-Aldrich Chemistry products. In this work, we used ZOC local product of PSTA synthesized from the zircon sand of Kalimantan. The synthesis of ZOC was carried out in the fluidized bed reactor by using chlorine gas and carbon at 1100 °C. The product of ZrCl₄ obtained was hydrolyzed to form ZOC [13-14].

In this research characterization and identification of ZrO₂-montmorillonite material made in PSTA-BATAN have been performed. The concentration of Zr interrays entering the montmorillonite interlayer was followed by UV-Vis DRS spectroscopy and XRD [15] [16]. The functional groups were performed with FTIR spectrophotometry while the porous distribution was observed by the BET method [17-18].

EXPERIMENTAL SECTION

Materials

In this research Na-montmorillonite type from Thailand was used, ethylene glycol pa, glycerol pa, each of which were made by E-Merck. Two types of intercalate solutions each of which from local ZrOCl₂.8H₂O (ZOC) (made of PSTA-BATAN) [13] were dissolved into 100 mL deionized water such that there were two series with concentrations of 0.1 , 0.2, and 0.5 M Zr and were added by ethylene glycol pa, 50 mL of glycerol pa stirred for 3-4 h and left overnight.

Instrumentation

Diffuse Reflectance Ultraviolet-Visible spectroscopy (UV-Vis DRS) ISR-2600Plus type and Fourier Transform Infrared spectroscopy (FTIR) IRTracer-100 type each of which are made by Shimadzu. A set of X-ray diffraction (XRD)-6000, Surface area analyzer Nova1000 and Transmission Electron Microscopy (TEM).

Procedure

Pillarization

One hundred gram (200 mesh) of Na-montmorillonite was weighed and put in a series of two beaker glass. Each series of which was added by two kinds of 500 mL intercalate solution, stirred and refluxed for 24 h [12]. The washing product was filtered, and washed with aquadest for several times on each intercalation product of 50 mL. The filtered products were divided into two parts, the first part for drying process with furnace at 105 °C for 5 h. While the second part was allowed to cool at room temperature till dry. Both types of drying products were calcined with variation of temperature, the calcination product was then called as the adsorbent material. Each of the calcination product was analyzed its functional groups properties with UV-Vis DRS, FTIR, BET, XRD and TEM instruments.

RESULT AND DISCUSSION

The entry of zirconium ions in the interlayer position of montmorillonite could be followed by the change of absorbance in the UV region of the DRS spectra or intensity of XRD. According to Vance [15] the intercalation concentration would be equivalent to the peak produced by DRS or XRD [11]. In Fig. 1 we can see the change of peak ZrO₂-montmorillonite image as a function of concentration.

From Fig. 1, it can be shown that the XRD and DRS image of ZrO₂-montmorillonite as a function of Zr concentration. It turns out that the greater concentration of Zr will result in an increase in absorbance or intensity of 2θ significantly, but at a concentration of 0.5 M the absorbance or at intensity 2θ of XRD decreased. This was likely the occurrence of re-desorption Zr into the liquid phase due to the swelling process was too big. This was in accordance with Chaabene statement [12], that excessive swelling process will cause the intercalant desorption to be greater. From Fig. 1, the concentration of 0.1–0.2 M Zr as the intercalant has been optimum.

The main disturbance to intercalation techniques using Zr⁴⁺ ion intercalant was the formation of aquo Zr-

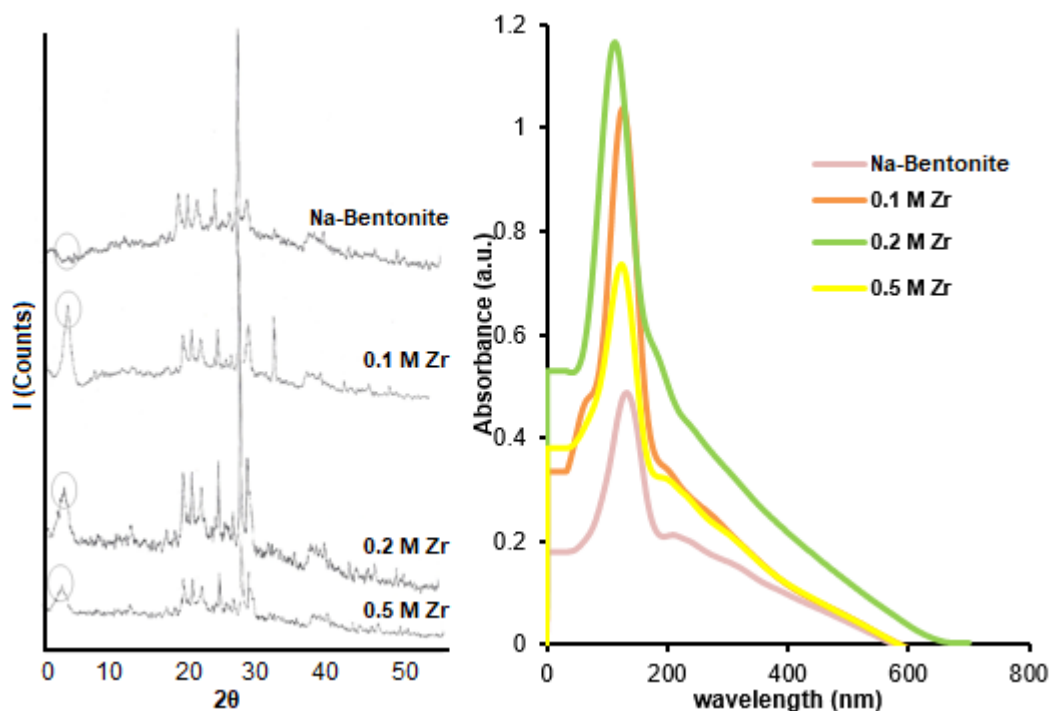


Fig 1. Image of XRD and DRS on ZrO_2 -montmorillonite as a function of Zr concentration

tetramer complex $[Zr_4(OH)_{14}(H_2O)_{10}]^{2+}$ at pH 6–7 [12]. The aquo complex was a polymer and has a large molecular weight. So to break it, the aquo complex must be prevented by the addition of a hydrophilic organic compound and often called a precursor. The compound of aquo Zr-tetramer complex $[Zr_4(OH)_{14}(H_2O)_{10}]^{2+}$ will break into Zr^{4+} ions when it was added by an hydrophilic organic compounds or heated above the temperature of $80\text{ }^\circ\text{C}$ [12].

In Fig. 2 is shown DRS peak image as a function of two types of warm and cold state precursors (room temperature) [11].

In Fig. 2, it could be shown the image of DRS on the intercalation quality of the ZrO_2 -montmorillonite expressed as the increase in absorbance. It was proven that the absorbance of the two precursors allowed to be at room temperature (cold) will have a higher absorbance value than that of the precursor which was being heated (hot). It is possible at high temperature not only break down Zr-tetramer complex $[Zr_4(OH)_{14}(H_2O)_{10}]^{2+}$ but also damage the montmorillonite interlayer lattice. As a result the pillared Zr^{4+} ion was getting more little and DRS absorbance peak decreased [12].

The image of absorbance increase of DRS in Fig. 2 shows that the precursor of ethylene glycol has higher absorbance than that of glycerol. This means that ethylene glycol is able to break down Zr-tetramer complex $[Zr_4(OH)_{14}(H_2O)_{10}]^{2+}$. While ethylene glycol also facilitates the pillarization process of Zr^{4+} ion by replacing

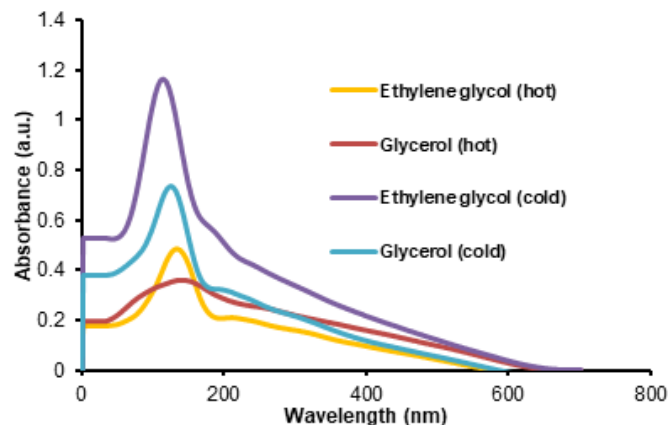


Fig 2. Influence of precursor on the image of DRS ZrO_2 -montmorillonite

other parent metal ions by exchanging of cations [19].

Furthermore, the pillarization technique, though it has experienced drying treatment at $110\text{ }^\circ\text{C}$, but it has a lot of content of small water and precursor and ZrO_2 found between interlayers was less orderly organized. Therefore, it was urgently so organize that Zr as interlayer pillar would be more perpendicular which meant that the new material of ZrO_2 -montmorillonite to be more porous [20].

In Fig. 3, it can be shown that the calcination process in ZrO_2 -montmorillonite would result in a wavelength shift from 150 nm to 300 nm by comparing Fig. 2 and 3. This means that the ZrO_2 molecule in the

montmorillonite lattice has been orderly better organized. Calcination would result in a loss of both water content as well as a precursor and a ZrO_2 molecule to be a pillar between the montmorillonite layers. The authors agree with LI Xiaoyun [21] that the consequences of the calcining process the material become more porous and the functional groups increases. In Fig. 3, it was seen the existence of an anomaly at a temperature of 800 °C the absorbance value decreases. This means that calcination will be maximum at the temperature of 600 °C, while at 800 °C the interlayer structure was predicted to be damaged.

In Fig. 4, it can be shown that the TEM image from the calcination effect of ZrO_2 -montmorillonite at 600 °C. It can be shown that before calcination (A) has a dark-looking surface image and its porosity was unrealistic. While the TEM image after calcination at temperature of 600 °C appears clear and was more porous than that of 400 °C [22].

Next, the surface area per gram sample of the calcined product (Fig. 3) was further calculated by using BET method (Brunauer-Emmett-Teller) as follows [23]:

$$1/[W(P/P_0)-1] = 1/W_m \times C + (C-1)/(W_m \times C) \times (P/P_0) \quad (1)$$

Notation of W is the adsorbed N_2 gas, P/P_0 relative pressure, W_m is the adsorbate weight as monolayer and C is the BET constant. The BET equation will be linear if plot $1/[W(P/P_0)-1]$ against P/P_0 , with slope (s) = $C-1/W_m$ x C and Intercept (i) = $1/W_m$ x C .

Furthermore, the surface area (St) (m^2) was calculated by $St = W_m \times N \times A_{cs}$, while the specific surface area (S) (m^2/g) was determined by dividing the sample capacity weight (W) of the monolayer state $S = St/W$. Notation of N as the Avogadro number (6.023×10^{23} molecules/mole), M as the adsorbate weight and A_{cs} cross sectional area (16.2 \AA for nitrogen) in $m^2/molecule$.

The result of the measurement of the BET sample as a function of the calcination temperature can be shown in Fig. 5. It turns out that the plot curve between plot $1/[W(P/P_0)-1]$ versus P/P_0 resulted three curves which were linear enough with all of those three correlation coefficient (r) were around 0.9980. On the measurement of surface area and specific surface area

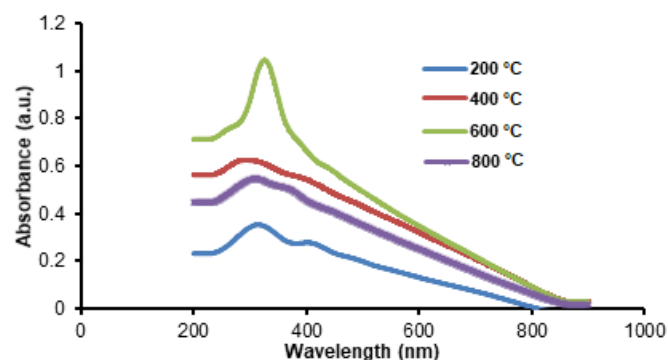


Fig 3. DRS image on the calcination effect of ZrO_2 -montmorillonite

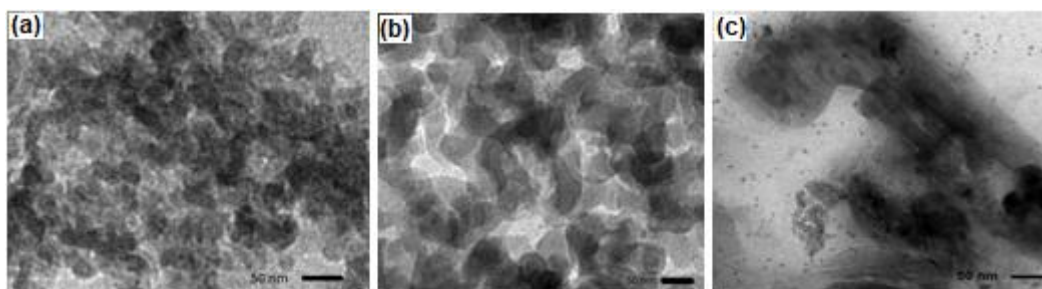


Fig 4. TEM image on the effect of calcination on ZrO_2 -montmorillonite at (a) before 600 °C and (b) after 600 °C (c) after 400 °C

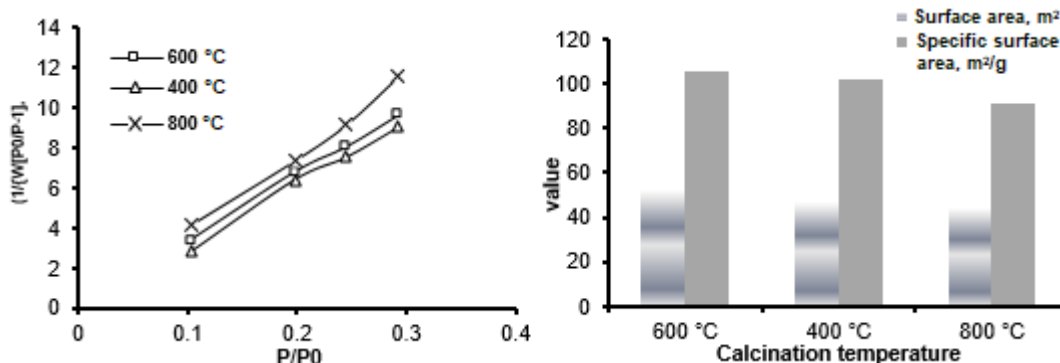


Fig 5. BET results as a function of calcination temperature

turns out the best value was achieved at calcination of 600 °C. This sense was supported by data that the TEM image was more porous (Fig. 4) at the calcination of 600 °C than that of 400 °C. In the following Fig. 6 the comparison of porous distribution between calcination products based on pore area versus radius by BET data method. In Fig. 6 it can be shown that the calcined sample at 600 °C was more likely porous in its meso pore region (< 50 nm) than that of the calcined sample at 400 °C. It is probably that the calcination sample at 600 °C was estimated to be more compacted, because Zr atoms would be more evenly pillarized.

Furthermore, the success of the pillarization technique was also characterized by the number of -OH stretching in the pillar group, as shown in Fig. 4 in which the detection of the -OH stretching functional group by using FTIR [16].

In Fig. 7, it was shown that the identification of the quality types were in the area of 3500–500 cm⁻¹. It turns out that two peaks are OH-stretching areas which are hydroxyl of the silanol group ($\equiv\text{Si-OH}$) especially in the areas contained in the external layer. While in 3626 cm⁻¹ can be interpreted as an $\equiv\text{Al-OH}$ group within the octahedral layer structure. This phenomenon answers the anomaly of why calcination at 800 °C, the DRS absorbance image decreases (Fig. 3). At the calcination of 800 °C, there was one peak in the area 3500–3740 cm⁻¹ or precisely at 3740 cm⁻¹ and there was no peak at 3650 cm⁻¹. This indicates that most of the

cluster of $\equiv\text{Al-OH}$ group on the interlayer suffered structural damage and resulted in a decrease in DRS absorbance and intensity of XRD.

While the stretching vibration of the water was identified as the -OH peak at 3425 cm⁻¹. The occurrence of the pillarization process caused by calcination could be identified as the number of -OH groups. The next peak around 1636 cm⁻¹ was the vibrational bond of water. The pillarization process which places a large amount of Zr on the interlayer would be hydrate-shaped which will decrease the intensity

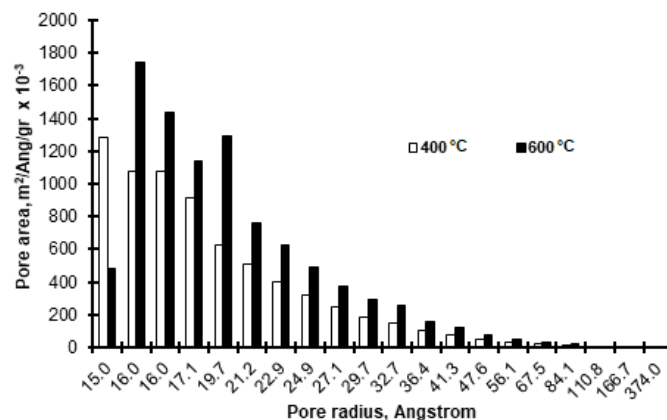


Fig 6. Porous distribution between the calcination products at 400 °C and 600 °C

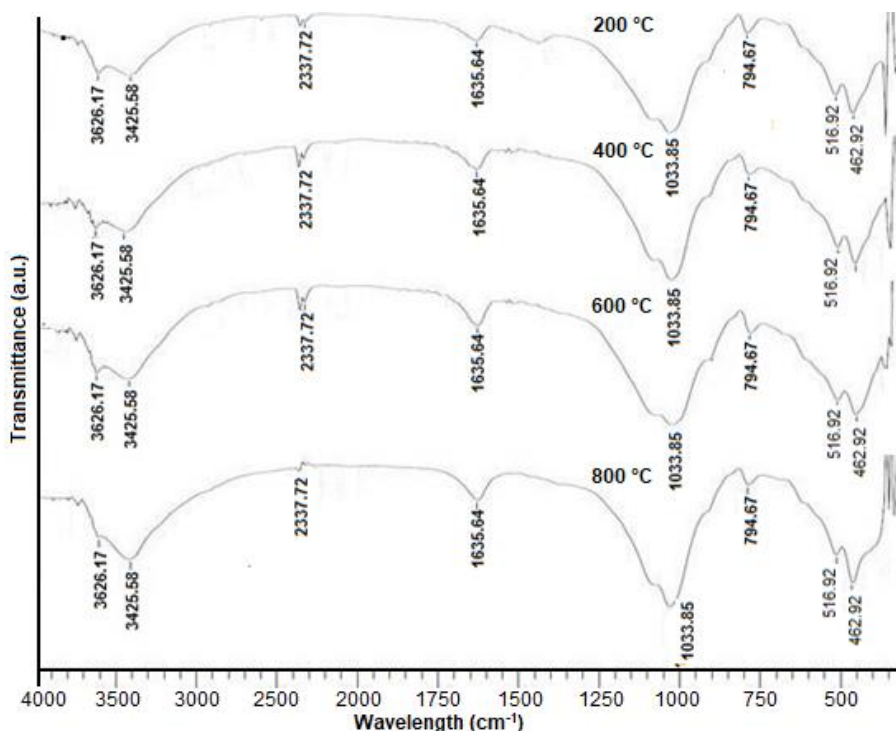


Fig 7. Calcined of FTIR image on ZrO₂-montmorillonite

of -OH at 1635 cm^{-1} . Then peak between 1033 cm^{-1} was the vibrational stretching asymmetry of tetrahedral SiO_2 , while 516–462 cm^{-1} were a functional vibration group of Si-O . The researcher agrees with the interpretation purposed by Suseno [24] on his research on the reactivity of the SiO_2 functional group. Thus with the existence of cluster of those Si-OH , Al-OH and Si-O functional groups, as the chemical reaction in the surface could be applied as the catalyst.

CONCLUSION

The new ZrO_2 -montmorillonite material from the local ZOC PSTA with Na-montmorillonite could be made through the pillarization process. The success of pillarization was determined by the image quality of the increase of absorbance of the UV-Vis DRS and of intensity at 5 angle 2θ of XRD. The best result of pillarization was obtained at Zr concentration of 0.2 M. The best precursor used was ethylene glycol with cold-drying process. The best calcining process at temperature of 600 $^\circ\text{C}$ with the absorbance value reached 1.3 au. The results of TEM and BET image observation after the calcination at temperature of 600 $^\circ\text{C}$, appeared clearer and more porous and have the specific surface area of 105 m^2/g . Obviously the result of interpretation using FTIR on ZrO_2 -montmorillonite contains the cluster of Si-OH , Al-OH and Si-O functional groups as pillar groups.

ACKNOWLEDGEMENT

With the completion of this paper, the authors express many thanks to Ir. Prayitno as the person in charge of SIPL and Iman Prayogo, S.Si., who has assisted us to solve the laboratory works and analysis. Furthermore, the authors are also very grateful to Deris Selawati and Yenni Rakhmawati as Labwork practicing Chemistry students of Faculty of Mathematics and Natural Sciences (PKL FMIPA Kimia UGM) who have been helpful in conducting this research.

REFERENCES

- [1] Poernomo.H., 2014, *Business prospect of local zircon sand becomes zirconium and radioactively free of rare earth metal oxide products*, the report of List of Budget Implementation, PSTA-Badan Tenaga Nuklir Nasional-Yogyakarta.
- [2] Muzakky, and Supriyanto, C, 2016, Modification of three types of bentonite with zirconium oxide chloride (zoc) of local products using intercalation process, *Indones. J. Chem.*, 16 (1), 14–19.
- [3] Mnasri, S, and Frini-Srasra, N., 2013, Synthesis, characterization and catalytic evaluation of zirconia-pillared bentonite for 1, 3-dioxalane synthesis, *Surf. Eng. Appl. Electrochem.*, 49(4), 73–84.
- [4] Fatimah, I., Wijaya, K., and Setyawan, K.H., 2008, Synthesis ZrO_2 -montmorillonite and application as catalyst in catalytic cracking of heavy fraction of crude oil, *BCREC*, 3 (1-3), 9–13.
- [5] Fatimah, I., Preparation of $\text{ZrO}_2/\text{Al}_2\text{O}_3$ -montmorillonite composite as catalyst for phenol hydroxylation, 2014, *J. Adv. Res.*, 5 (6), 663–670.
- [6] Fatimah, I., Rubiyanto, D., Huda, T., Handayani, S., Ilahi, O.M., and Yudha, S.P., 2015, Ni dispersed on sulfated zirconia pillared montmorillonite as bifunctional catalyst in eco-friendly citronellal conversion, *Eng. J.*, 19 (5), 43–53.
- [7] Fatimah, I., Rubiyanto, D., and Kartika, N.C., 2016, Effect of calcination temperature on the synthesis of ZrO_2 -pillared saponite to catalytic activity in menthol esterification, *Indones. J. Chem.*, 16 (1), 8–13.
- [8] Utubira, Y., Wijaya, K., Triyono, and Kunarti, E.S., 2016, Microwave assisted preparation of zirconia-pillared bentonite, *Int. J. ChemTech Res.*, 9 (4), 475–482.
- [9] Bahranowski, K., Włodarczyk, W., Wisła-Walsh, E., Gaweł, A., Matusik, J., Klimek, A., Gil, B., Michalik-Zym, A., Dula, R., Socha, R.P., and Serwicka, E.M., 2015, [Ti,Zr]-pillared montmorillonite – A new quality with respect to Ti- and Zr-pillared clays, *Microporous Mesoporous Mater.*, 202, 155–164.
- [10] Suseno, A., Wijaya, K., Trisunaryanti, W., Roto, and Priyono, 2017, The textural properties of Zirconia pillared Indonesian bentonite, *Int. J. ChemTech Res.*, 10 (2), 40–44.
- [11] Chaabene, S.B., Bergaoui, L., and Ghorbel, A., 2004, Zirconium and sulfated zirconium pillared clays: A combined intercalation solution study and solid characterization, *Colloids Surf., A*, 251 (1-3), 109–115.
- [12] Budi, S., 2005, Pembuatan zirkon Tetraklorida dari pasir zirkon dengan proses kering secara langsung, *Jurnal Iptek Nuklir Ganendra*, 8 (1), 15–22.
- [13] Tuyen. N.V., Quang, V.T., Huong, T.G., and Anh, V.H., 2007, Preparation of high quality zirconium oxychloride from zircon of Vietnam, *VAEC Ann. Rep.*, 7 (43), 286–291.
- [14] Vance, E.R., Zhang, Y., and Zhang, Z., 2010, Diffuse reflectance and X-ray photoelectron spectroscopy of uranium in ZrO_2 and $\text{Y}_2\text{Ti}_2\text{O}_7$, *J. Nucl. Mater.*, 400 (1), 8–14.
- [15] Rinaldi, N, and Kristiani, A., 2017, Physicochemical of pillared clays prepared by several metal oxides, *AIP Conf. Proc.*, 1823,

- 020063.
- [16] Cecilia, J.A, García-Sancho, C., and Franco, F., 2013, Montmorillonite based porous clay heterostructures: Influence of Zr in the structure and acidic properties, *Microporous Mesoporous Mater.*, 176, 95–102.
- [17] Elkhalfah, A.E.I., Maitra, S., Bustam, M.A., and Murugesan, T, 2013, Effects of exchanged ammonium cations on structure characteristics and CO₂ adsorption capacities of bentonite clay, *Appl. Clay Sci.*, 83-84, 391–398.
- [18] Salem, .S., Salem, .A., and Babaei, A.A., 2015, Preparation and characterization of nano porous bentonite for regeneration of semi-treated waste engine oil: Applied aspects for enhanced recovery, *Chem. Eng. J.*, 260, 368–376.
- [19] Feng, Y., Li, X., Xu, K., Zou, H., Li, H., and Liang, B., 2015, Qualitative and simultaneous quantitative analysis of cimetidine polymorphs by ultraviolet-visible and shortwave near-infrared diffuse reflectance spectroscopy and multivariate calibration models, *J. Pharm. Biomed. Anal.*, 104, 112–121.
- [20] Zheng, Y., Liu, J., Hu, Q., and Cai, Q., 2014, Study on microstructure of muddy intercalation using SEM method, *Electron. J. Geotech. Eng.*, 19, 9953–9963,.
- [21] Muzakky, Wijaya, K., and Prayogo, I., 2013, Zirconia-intercalated bentonite as catalyst candidate I: Preparation and characterization of [Zr₄(OH)₁₄(H₂O)₁₀]²⁺ intercalated bentonite, *Int. J. Appl. Chem.*, 9 (3), 243–252.
- [22] Suseno, A., Wijaya, K, Trisunaryati, W., and Shidiq, M., 2016, Synthesis and characterization of ZrO₂-pillared bentonites, *Asian J. Chem.*, 27 (7), 2619–2623.